UNIVERSITY OF BEIRA INTERIOR

UBI
Covilhã
Portugal

Thermodynamic Analysis and Optimization of a Scramjet Engine with Thermal Management System

Luís Rodrigues

Supervisor

Prof. Dr. Francisco Brójo

This thesis is submited to University of Beira Interior
in partial fulfilment of the requirements for the degree of Master of Science

Faculty of Engineering
Department of Aerospace Sciences

June 26, 2010

Declaration of Authorship

I, Luís Rodrigues, declare that this thesis titled, 'Thermodynamic Analysis and Optimization of a Scramjet Engine with Thermal Management System' and the work presented in it are my own. I confirm that:

- This work was done wholly or mainly while in candidature for a research degree at this University.
- Where any part of this thesis has previously been submitted for a degree or any other qualification at this University or any other institution, this has been clearly stated.
- Where I have consulted the published work of others, this is always clearly attributed.
- Where I have quoted from the work of others, the source is always given. With the exception of such quotations, this thesis is entirely my own work.
- I have acknowledged all main sources of help.
- Where the thesis is based on work done by myself jointly with others, I have made clear exactly what was done by others and what I have contributed myself.

Signed: _____

Date: _____

“For once you have tasted flight you will walk the earth with your eyes turned skywards, for there you have been and there you will long to return.”

Leonardo da Vinci

UNIVERSITY OF BEIRA INTERIOR

Abstract

Faculty of Engineering
Department of Aerospace Sciences

Masters in Aeronautical Engineering

Elaborated by Luís Rodrigues

Thermal management of the scramjet engine is one of the key issues of the challenges brought by the development of hypersonic airbreathing vehicles. A Closed Brayton Cycle thermal management system for a regenerative cooled scramjet is introduced with the goal of reducing the hydrogen fuel flow for cooling. Part of the heat absorbed from fuel is converted into other forms of energy to decrease the heat that must be taken away by hydrogen fuel. Reducing this heat increases the fuel heat sink (cooling capacity) without requiring excess fuel for cooling and eliminating the need to search for a new coolant. The proposed thermal cycle reduces the fuel flow for cooling, and this way, the fuel on board assures the cooling requirements for the whole hypersonic vehicle. The basic concept and working principle are introduced: a thermodynamic cycle analysis is performed to demonstrate the system performance gains of Closed Brayton Cycle (CBC) Thermal Management System (TMS) over the conventional system with regenerative cooling. It was shown that the Closed Brayton Cycle Thermal Management Systems presents a high performance gain when compared to conventional regenerative cooling due to the reduction of fuel flow for cooling and additional power output.

(Keywords: Scramjet, Regenerative Cooling, Thermal Management System, Heat Sink.)

UNIVERSITY OF BEIRA INTERIOR

Resumo

Faculty of Engineering
Department of Aerospace Sciences

Masters in Aeronautical Engineering

Elaborated by Luís Rodrigues

A evolução dos veículos hipersónicos despoletou diversos desafios, sendo a gestão térmica de um motor scramjet um dos tópicos principais. É apresentado um sistema de gestão térmica designado Closed Brayton Cycle para um motor scramjet regenerativamente arrefecido.
Com o objectivo de reduzir o fluxo de combustível para refrigeração do motor e simultaneamente a quantidade de calor que necessita de ser eliminada, uma parte do calor absorvido pelo combustível é convertido em diferentes formas de energia. A redução do fluxo de combustível significa um aumento da capacidade de refrigeração.
A necessidade de recorrer a quantidades extra de combustível é eliminada, assim como a necessidade de desenvolvimento de um novo refrigerante. Através da redução do fluxo de combustível para refrigeração, o combustível a bordo da aeronave garante os requisitos de refrigeração para todo o veículo hipersónico. O conceito básico e o principio de operação são apresentados, uma análise termodinámica é efectuada para demonstrar o desempenho do sistema Closed Brayton Cycle relativamente ao sistema convencional com arrefecimento regenerativo. Foi demonstrado que o sistema Closed Brayton Cycle apresenta um ganho de desempenho alto quando comparado com o sistema regenerativo convencional devido à redução do fluxo de combustível e devido também à potência adicional gerada.

(Palavras chave: Scramjet, Arrefecimento regenerativo, Sistema de gestão térmica, Capacidade de arrefecimento.)

Acknowledgements

I would like to thank Prof. Dr. Francisco Brójo for his imense patiente and diligence. Without his guidance this project would not have been possible.

I would like to thank Prof. Dr. Kouamana Bousson for his support and guidance which was essential to the realization of this project.

I want to thank my family for their love and support through out the years.

Finally, I want to give a big kiss to my parents for their endless love and support, I owe them everything.

Contents

List of Figures

List of Tables

Nomenclature

C_P	Specific heat of fuel	kJ/(kg K)
C_F	Heat capacity rate of high-temperature heat source	kW/K
C_L	Heat capacity rate of low temperature heat sink	kW/K
C_{wf}	Heat capacity rate of the working fluid	kW/K
D	Total pressure recovery coefficient	
ε_H	high-temperature side heat exchanger validity	
ε_L	low-temperature side heat exchanger validity	
h'_{fc}	Indirect heat sink	kJ/kg
h_{fc}	Actual heat sink	kJ/kg
m_1	Fuel flow rate for regenerative cooling	kg/s
m_2	Fuel flow rate thermal management system	kg/s
Δm	Fuel flow saving ratio	
Q_1	Heat transfer amount of wall 1	kW
Q_2	Heat transfer amount of low temperature heat exchanger	kW
Q_3	Heat transfer amount of wall 2	kW
T_W	High temperature heat source	K
T_0	Entrance temperature of fuel at cooling passage	K
T_3	Exit temperature of fuel at cooling passage	K
T_5	Exit temperature of fuel at low-temperature heat exchanger	K
W	Available work of cycle	kW
$\overline{W}$	Non-dimensional power	

γ	Adiabatic index
χ	Isentropic temperature ratio
η	Cycle efficiency
η_c	Efficiency of compressor

η_t	Efficiency of turbine
δ	Multiplication ratio of fuel heat sink
π	Pressure ratio of compressor

Chapter 1

Introduction

1.1 Motivation

The interest in airbreathing propulsion vehicles is traced back many decades. Attractive as propulsive devices due to their ability to uphold high speeds atmospheric flight, there has been a rebirth of research activity as a result of the significant performance improvements acquirable through the advancement of the underlying technologies. One of the key issues hypersonic flight addresses is the thermal management of the overall vehicle and more specifically the cooling of the scramjet engine. Composite materials cannot withstand the large load in a scramjet combustion chamber, and by so, regenerative cooling assumes an important role. The increase of the flight speed to high supersonic and hypersonic regime, makes it necessary to use fuel as primary coolant once the ram air temperature taken on board the vehicle become too high to cool the structure. Fuel flows through the cooling passage to cool the engine walls before it is used for combustion. Beyond certain Mach number, the stoichiometric flow rate is exceeded by the coolant flow rate, hence, the fuel heat sink is insufficient. This implies that more fuel must be carried than the required for executing the mission, and that excess fuel must be abandoned. The additional fuel will mean extra hardware which will increase size, weight and complexity to the vehicle, degrading the vehicle performance. Furthermore, lack of heat sink limits the hypersonic vehicle to a relatively low flight speed. In an opposing way to conventional aero-engines, where cooling air as low-temperature heat source is considered infinite, the amount of fuel onboard for cooling the scramjet is very limited. Hence, the low-temperature heat source for scramjet is finite. If the low-temperature heat source needs could be improved, the cooling requirement might be achieved. A Closed Brayton cycle (CBC) thermal management system (TMS) based on the thermodynamic principle arises as an alternative to the effective use of the limited resources available to reduce the fuel flow needed for cooling. In this system, other coolant is introduced as primary coolant, and fuel is used as secondary cooling. Since part of the heat is transformed to other forms of energy, the ultimate heat needed to be taken away by hydrogen fuel decreases, reducing the fuel flow needed for cooling.

1.2 Definition of Scramjet

First, it is necessary to understand the definition of a ramjet engine, as a scramjet engine is a direct successor of a ramjet engine. Ramjet engines are characterized for having no moving parts. The compression is achieved at the air intake by the forward speed of the vehicle. Basically, air entering the intake of a supersonic aircraft is slowed by aerodynamic diffusion at the inlet and diffuser to velocities comparable to those in a turbojet compressor. Furthermore, the exhaust air is accelerated to a higher velocity than that of the inlet through the expansion of hot gases after the injection and burn of fuel, and by so is created a positive push.

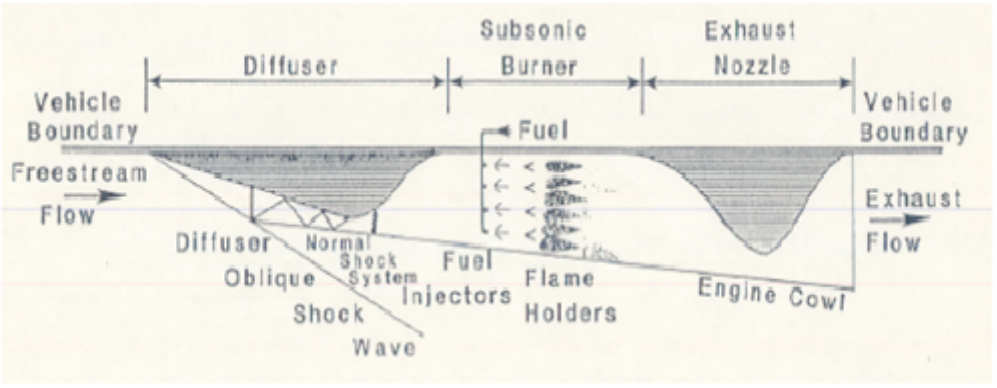

FIGURE 1.1: Two-dimensional Schematic of a Ramjet Engine.
[1]

The pressure, temperature and density of the flow entering the burner are significantly larger than in the freestream due to the deceleration of the freestream air. For Mach numbers beyond Mach 6 it becomes inefficient to slow to subsonic speeds. Thus, if the flow is no longer slowed to subsonic speeds, but rather only slowed to acceptable supersonic speeds, the ramjet is then themed a 'supersonic combustion ramjet'[1], resulting in the acronym scramjet.

To summarize, a scramjet engine (see Figure 1.2) can be described as a hypersonic air-breathing engine in which heat addition occurs in a flow that is supersonic relative to the engine, due to the combustion of fuel in air. The airflow in a pure scramjet remains supersonic throughout the combustion process and does not require a chocking mechanism. Currently, scramjet engines are able to seamlessly make the transition between ramjet and scramjet operation.

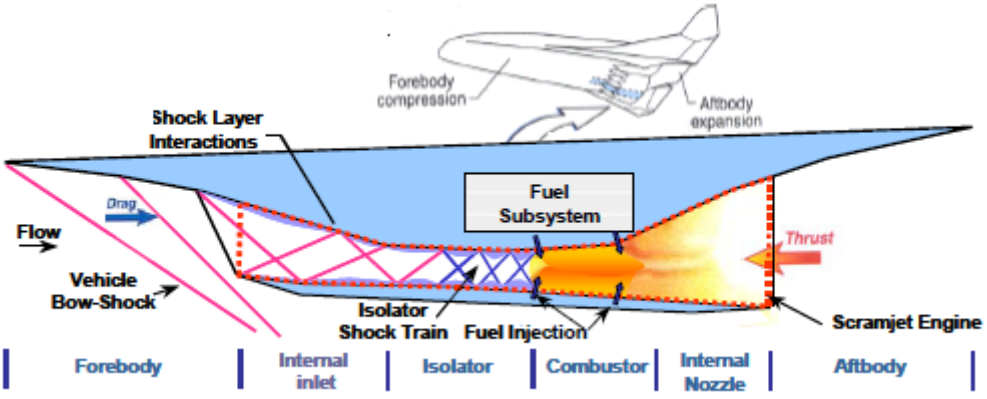

FIGURE 1.2: Representative Schematic of a Scramjet Engine. [2]

1.3 Scramjet Aerodynamics

Geometrical configuration and design represent the most important requirements to understand hypersonic air-breathing engines aerophysics. The scramjet engine occupies the entire lower surface of the vehicle body. Scramjet propulsion system consists of five major engine components: internal inlet, isolator, combustor, internal nozzle and the fuel supply subsystem. The vehicle forebody composes an essential part of the air induction system, on the other side, the vehicle afterbody represents a critical part of the nozzle component. These are schematically described in Figure 1.2. High-speed air induction system, composed by the vehicle forebody and internal inlet has the main objective of capturing and compressing air. While in a conventional jet engine, inlet and mechanical compressor work in combination to provide the necessary high pressure to the entire engine, for supersonic and hypersonic vehicles, adequate compression can be achieved without a mechanical compressor. Initial external compression is provided by the forebody and it contributes to the drag and moments of the vehicle. The final compression of the propulsion cycle is achieved through the internal inlet compression. Together with the internal inlet, the forebody is drafted to provide the required mass capture and aerodynamic contraction ratio at maximum inlet efficiency. The air in the captured stream tube suffers a reduction in Mach number along with an increase in pressure and temperature as it passes through the system of shock waves in the forebody and internal inlet. The combustion process can be affected by the non-uniformities, resultant of the oblique reflecting shock waves[2] (see Figure 1.3). Scramjet air induction phenomena includes vehicle bow shock and isentropic turning Mach waves, shock-boundary layer interaction, non-uniform flow conditions, and three-dimensional effects[2].

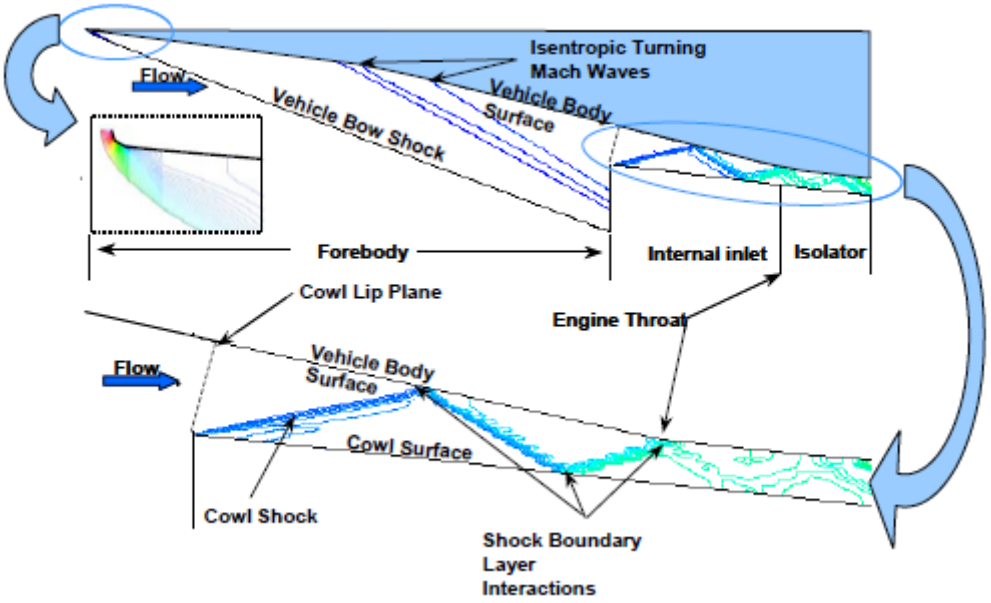

FIGURE 1.3: Important Forebody and Internal Inlet Physics.
[2]

The isolator allows supersonic flow to adjust to a static backpressure higher than its inlet static pressure[2]. To settle the boundary layer separation the isolator cross-sectional area may be slightly divergent or constant. When the boundary layer starts to separate, due to the combustion process, a pre-combustion shock is formed (see Figure 1.4). The shock train enables the required pressure rise to occur over a finite distance, isolating the combustion process from the inlet compression process, therefore acting to prevent inlet surge or unstart. Isolator length is defined as the necessary length to capture the pressure rise. The isolator in a dual mode ramjet and scramjet is a vital component that allows the combustor to achieve the required heat release profile and capture the induced combustor pressure rise without inlet unstart. It also enables the engine to complete the transition to scramjet operation.

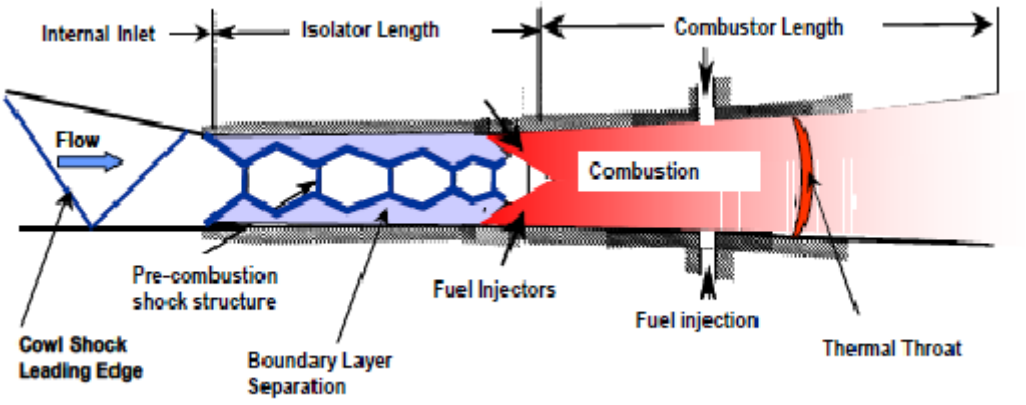

FIGURE 1.4: Isolator and Combustor Physics.
[2]

The combustor captures the inlet/isolator airflow with variations in geometry inflow profiles and provides efficient fuel air mixing within the available combustor length as illustrated in Figure 1.4. To deliver fuel

to the flowpath at appropriate locations with the desired physical properties a fuel supply subsystem is needed. The combustor fuel is programmed to stay within the engine operability limits while optimizing engine thrust potential. The expansion system (i.e, internal nozzle and vehicle aftbody), completes the propulsion flowpath and controls the expansion of the high pressure and temperature gas mixture to produce net thrust. During the expansion process, the potential energy generated by the combustor is transformed into kinetic energy. The nozzle must process the accumulated flow distortions generated by the air induction system, isolator and combustor. The important scramjet nozzle physical phenomena, as shown in Figure 1.5, addresses phenomenon's like flow chemistry, boundary layer effects, non-uniform flow conditions, shear layer interaction, and three-dimensional effects. The efficiency of the propulsion system and the vehicle is greatly affected by the nozzle design due to its ability to influence vehicle pitching moment and lift.

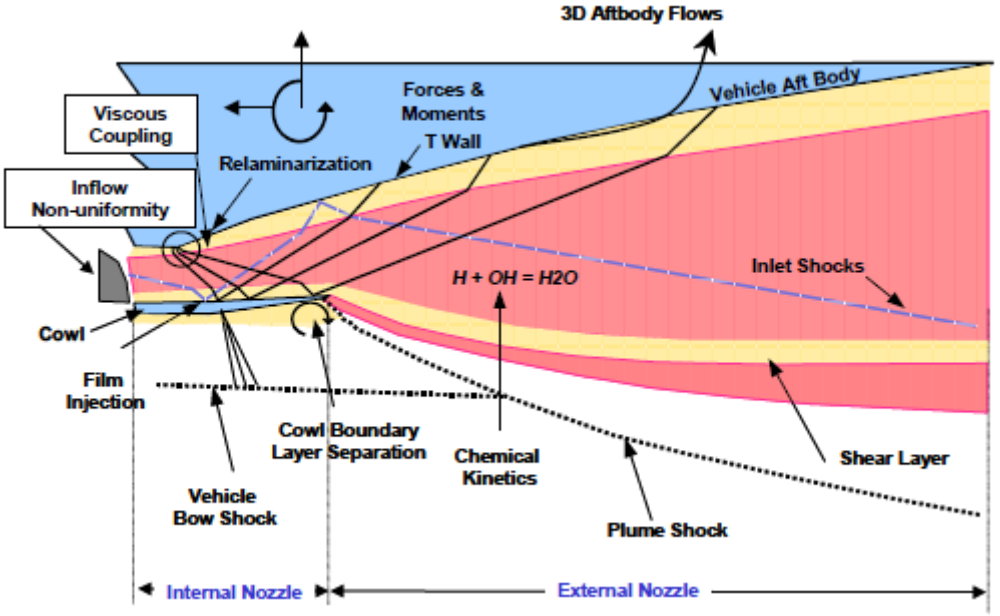

FIGURE 1.5: Summary of Important Scramjet Nozzle Physics. [2]

1.4 Operational Characteristics

An air-breathing hypersonic vehicle operates in multiple engine cycles and modes to reach scramjet operating speeds. A representative air-breathing hypersonic flight corridor with operational limits is illustrated in Figure 1.6. Thermal and structural limitations set the lower bound (generally at a dynamic pressure about $9.5764e^4$ Pa). The upper bound of the envelope is defined by combustion stability considerations, (typically at a dynamic pressure of $2.394e^4 - 4.788e^4$ Pa).

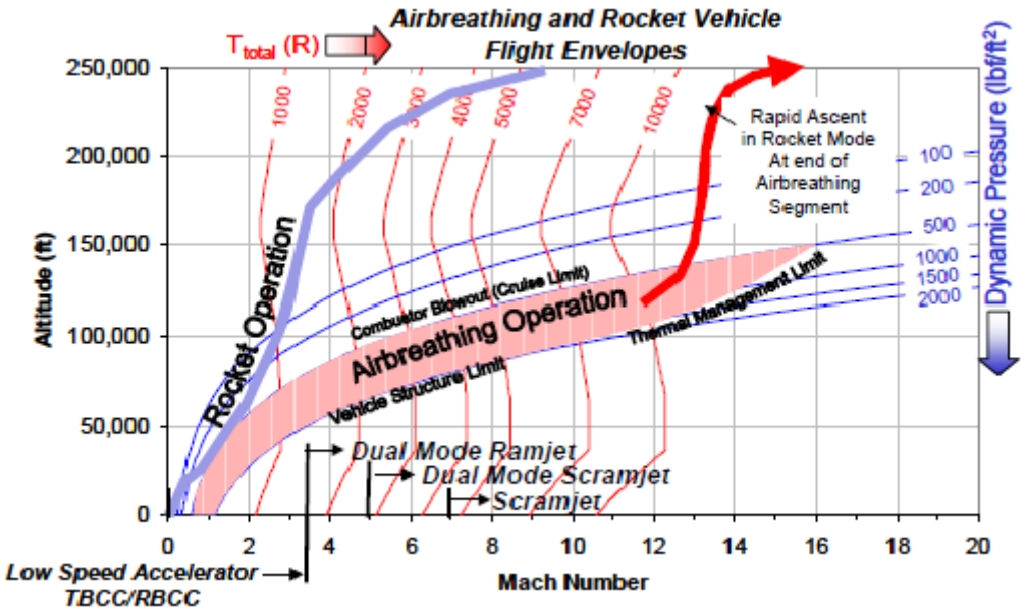

FIGURE 1.6: Air-breathing Hypersonic Vehicle Flight Trajectory and Operational Limits. [2]

In the range of flight Mach number 0 to 3 (low speed regime) several possible propulsion cycles may be used, such as, Turbine Based Combined Cycle (TBCC), consisting in a bank of gas turbine engines in the vehicle, or Rocket Based Combined Cycle (RBCC), with integrated rockets, internal or external to the engine, to accelerate the vehicle from takeoff to Mach 3.

In the Mach number range 3 to 4, the scramjet engine transitions from low speed propulsion cycles to dual mode ramjet combustion system. Dual-mode ramjet operation occurs when the terminal shock system (see Figure 1.4) is of sufficient strength to create a region(s) of subsonic flow at the entrance to the combustor[2].

In a conventional ramjet, by increasing the diffuser area, air is decelerated to low subsonic speeds ensuring that complete combustion process will occur at subsonic speeds. After the combustor, the converging-diverging nozzle creates a physical throat and generates the required engine thrust.

A scramjet engine synergistically designed to operate as dual mode ramjet and scramjet presents no physical throat between the combustor and expansion system providing an optimum cycle over a larger operating range. In the inner part of the combustor, the required choking is provided by means of thermal throat and can be achieved by correctly choosing the combination of area distribution, fuel air mixing and combustion efficiency, as represented by total temperature distribution.

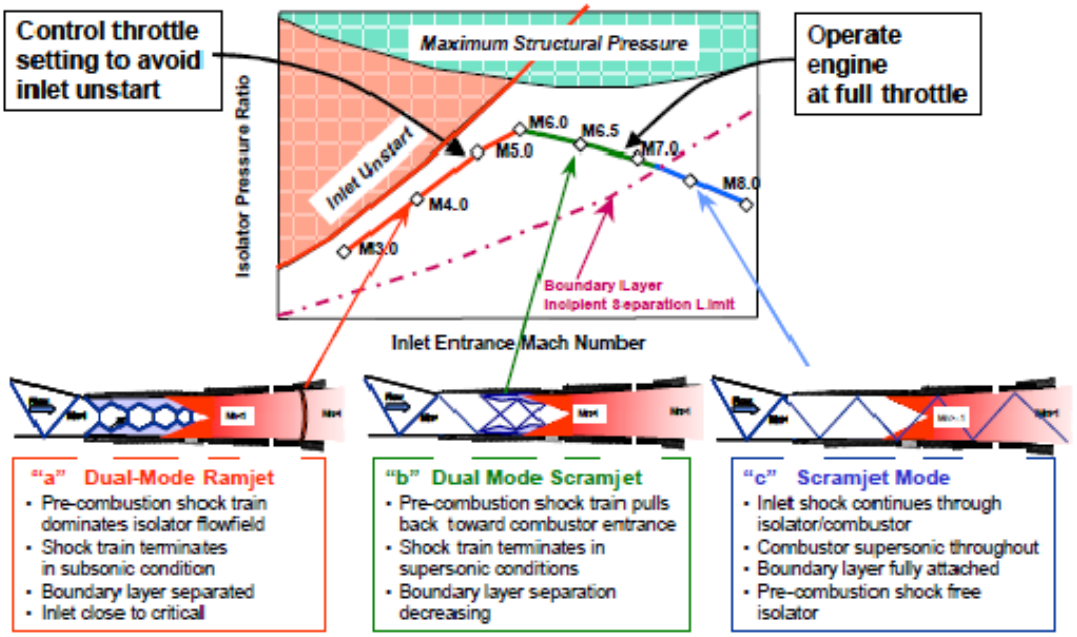

FIGURE 1.7: Isolator Provides Dual Mode Scramjet Seamless Transition to Scramjet. [2]

As the scramjet-powered vehicle accelerates from Mach 3 to 8, it initially operates as a dual-mode ramjet in the Mach 3 to 6 regime. In the flight region of Mach 5 to 7 the scramjet air-breathing propulsion system has a mid-speed transition region in which neither ramjet or scramjet mode is sufficient to describe the internal flow-field. The total temperature rise across the combustor begins to decrease along the pressure rise produced by the combustion process. Therefore, a weaker pre-combustion system is needed and the pre-combustion shock is pulled back from the inlet throat towards the entrance to the combustor. In this critical regime, scramjet operation is referred as dual-mode scramjet, where subsonic and supersonic flow characteristics are mixed or active transitioning between subsonic and supersonic combustion within the scramjet.

Beyond Mach 7, the combustion process cannot separate the flow and the engine operates in scramjet mode with a pre-combustion shock-free isolator. The inlet shocks propagate through the entire engine. Scramjet engines operational lines are illustrated in Figure 1.7.

1.5 General Background of Hypersonic Vehicles

Hypersonic airbreathing propulsion systems offer the potential to enable new classes of flight vehicles. The promising high-speed performance of the hydrogen fueled scramjet engine and more importantly its emerging potential for achieving near-orbital speeds, led to increased attention on hypersonic vehicles. Efficient airbreathing engines for operation into the hypersonic speed regime have been studied for over 40 years. The core of these engine systems is the supersonic combustion ramjet (scramjet) cycle.

Scramjet engine concept development, test facilities and instrumentation development, analysis method refinement, component and engine testing have been pursued continually since the early 1960s.

1.5.1 First Generation Scramjet Development (1960 - 1973)

In the early 1950s the interest in burning fuels in external streams to either reduce the base drag of supersonic projectiles or to produce lift and/or thrust on supersonic and hypersonic airfoils represented the origins of employing combustion to supersonic flows in the United States. Several interesting findings were provided by Dugger, in 1960, on the relative performance of kerosene-fueled conventional ramjet (CRJ) and was shown that the performance of a scramjet engine would exceed the performance of the CRJ in the speed range of Mach 6 to 8[3]. The year of 1960 represented as well the first scramjet demonstration, executed by Ferri. This demonstration was the starting point of several developing programs in the United States, the most extensive being held by NASA Hypersonic Research Engine or Hypersonic Ramjet Experiment (HRE). This program had the goal of developing and demonstrating flight-weight, variable geometry, hydrogen-fueled and cooled scramjet engine technology. 1960 represented as well the beginning of the Canadian interest in supersonic combustion, more accurate, in hypersonic inlet aerodynamics and gun launched scramjet flight testing. In Europe, throughout the 1960s and 1970s, that interest was paralleled.

1.5.2 Second Generation Scramjet Development (1973-1986)

The second generation represented the shift of interest, in the U.S, to the integration of hydrogen-fueled scramjet engines on a hypersonic vehicle. NASA Langley Research Center (LaRC) led this effort, with much of the research efforts being held on tool development, namely, facilities, test methodologies, cycle analysis, data analysis and computational fluid dynamics, CFD. Aerodynamic and propulsion-airframe integration (PAI) tests were performed to quantify inlet capture, external nozzle performance, and scramjet-powered vehicle performance.
During the mid-1970s, sidewall compression flowpath tests demonstrated the required thrust, operability and fuel cooling requirements to allow a trustworthy vehicle design.
In the late 1970s, scramjet module and direct-connect research and testing involving gaseous hydrogen fuels was developed by NASA LaRC but was interrupted by the NASP program. Ultimately, U.S. Air Force leaded research in this area, performing several tests using ethane, methane and ethylene injected from hydrogen fuel injectors.

1.5.3 Third Generation Scramjet Development (1986-1994)

U.S. NASP program, was in the early 1980s, developed with the objective of creating a single-stage-to-orbit 'hypersonic combined-cycle airbreathing capable' [3] engine, demonstrated by the research vehicle, X-30 (see Figure 1.8).

FIGURE 1.8: X-30 NASP National Aero-Space Plane.
[2]

The capacity of flying a single-stage vehicle, powered by a combined cycle engine that utilized scramjet operation up to Mach 25 was very aggressive considering the state of technology in 1984. At the time, no reliable scramjet engines performance, operability, loads, or structural approaches had been tested above Mach 7. In other words, second generation technology was a good starting point, but considerable refinement and development was needed.
Third generation scramjet development accommodated several advances starting at an international level with Germany development of Sänger II as a proposed two-stage-to orbit (TSTO) concept. Japan pursued the development of combined cycle engine technology for flyback booster TSTO applications. ORYOL program represented the debut of Russia in hypersonic research and development, through exploiting combined propulsion systems for advanced reusable space transportation. Finally, France presented PREPHA that aimed at developing a knowledge base on hydrogen-fueled dual-mode ramjet technology for STTO applications.

1.5.4 Fourth Generation Scramjet Development (1995-Today)

After the NASP program, the United States focused their attention in three new directions. NASA aeronautics aimed at demonstrating the most advanced parts of the NASP propulsion technology (Hyper-X), in other words, scramjets. As part of the Hyper-X program significantly modifications to the original engine design of the NASP program were made, and these modifications were used as the foundation to power plant the successful X-43A (see Figure 1.9) vehicle that flew at Mach 7 in March 2004. The

data provided by this flight is a major step towards the validation of hypersonic air-breathing vehicles and engine design methods[3].

FIGURE 1.9: Captive Carry-to-Launch Conditions and X-43A First Free Flight Scramjet. [2]

On the other side, NASA rocket community embraced the engine technology afforded by rocket-airbreathing combined cycle engines (Spaceliner program). U.S Air Force went back to hydrocarbon-fueled scramjet missiles (HyTech/HySet program). United States has since incorporated the development of high-speed airbreathing technology within and overarching approach called the National Aerospace Initiative (NAI). It was a partnership between the Department of Defense and NASA designed to sustain the U.S leadership through technology development and demonstration in three pillar areas of high speed/hypersonics, space access, and space technology. An extensive summary of the scramjet‘s evolution starting with its origin in 1955 through the year of 2004 and can be found in Tables A.1 and A.2 (see Appendix).

1.6 Applications of Scramjets

Scramjet engines address a wide range of possible applications, including missile propulsion, hypersonic cruiser propulsion and part of a staged space access propulsion system. Figure 1.10 displays the approximate performance range in terms of engine specific impulse and Mach number for several types of propulsion systems. For flight Mach number ranges from 6 to 7, the only suitable engines are rockets and scramjets. In comparison to rockets, scramjets have much higher specific impulse levels, therefore, it is explicit why it is advantageous to develop the scramjet. Furthermore, scramjets do not require that an oxidizer be carried on board of the aircraft as it is an airbreathing engine, collecting oxygen from the atmosphere, which implies a decrease on the required weight of the overall propulsion system and fuel resulting in a higher allowable payload weight or increased range. Others advantages of developing the airbreathing engine, are confined to the fact it has higher engine efficiency, enabling longer

powered range as well as it has the ability for thrust modulation to ensure efficient operation, higher maneuverability and are completely reusable.

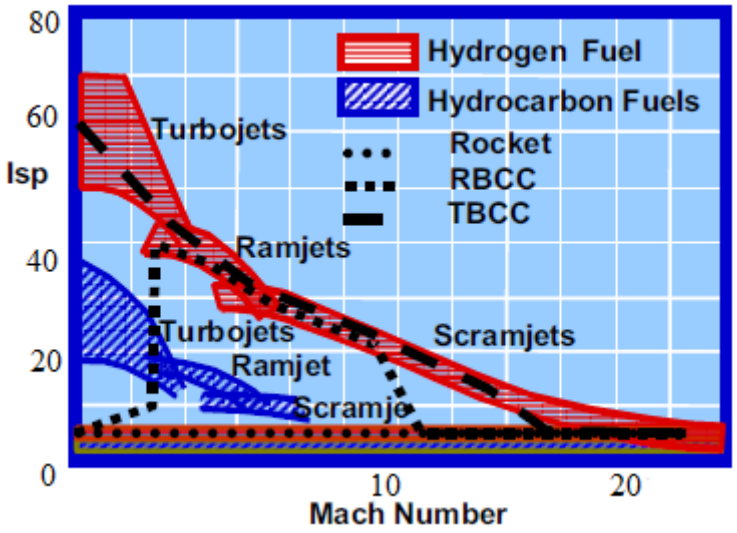

FIGURE 1.10: Specific Impulse Versus Mach Number for Various Engine Types.
[4]

1.6.1 Military and Civilian Applications

Military benefits of hypersonic vehicles are versatility, response time, survivability, and unfueled range. Civilian benefits are long range rapid commercial transportation and safe, affordable reliable and flexible transportation to low-earth orbit. One example of a potential hypersonic cruise military aircraft is the Aurora shown in Figure 1.11.

FIGURE 1.11: Aurora Mach 5 Reconnaissance Aircraft Configuration.
[5]

1.6.2 Space Launch Applications

Benefits of air-breathing launch systems are improved safety, mission flexibility, vehicle design robustness and reduced operating costs. Air-breathing vehicles, capable of hypersonic speeds, can transform access to space. Rocket-powered vehicles are approaching their limits in terms of these parameters, switching to a new approach is the only way to achieve significant improvements. Safety benefits result from characteristics such as enhanced abort capability and moderate power density. Horizontal takeoff and powered landing enables the ability to abort over most of the flight. High lift/drag (L/D) allows longer-range glide for large landing footprint. Power density, or the quantity of propellant pumped for a given thrust level, is 1/10 that of a vertical takeoff rocket due to lower thrust loading (T/W), lower vehicle weight and higher specific impulse. Power density is a large factor in catastrophic failures. Recent analysis indicates that safety increases by several orders of magnitude are possible using air-breathing systems. Mission flexibility results from horizontal takeoff and landing, the large landing (unpowered) footprint and high L/D. Utilization of aerodynamic forces rather than thrust allows efficient orbital plane changes during ascent, and expanded launch window. Robustness and reliability can be built into air-breathing systems because of large margins and reduced weight growth sensitivity, and the low thrust required for smaller, horizontal takeoff systems. Cost models indicate that about one-order magnitude reduction in operating cost is possible[6].

1.7 Fuel Choice

Heat-sink and vehicle system-level requirements dictates the fuel choice, between hydrocarbon and hydrogen (see Figure 1.12).

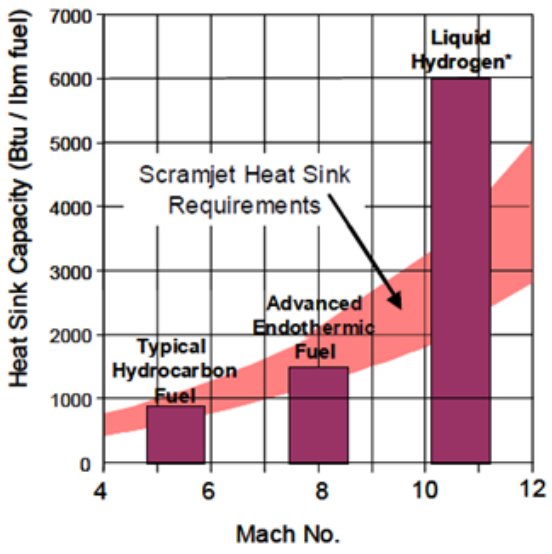

FIGURE 1.12: Heat Sink Capacity of Hydrocarbon and Hydrogen Fuels Relative to Scramjet Requirements.
[2]

Cryogenic hydrogen presents a much higher energy per unit mass, however, its smaller density means a significantly lower energy per unit volume when compared to several hydrocarbon derivatives (see Table 1.1). The higher specific impulse achievable through hydrogen propulsion makes this the better choice when hypersonic vehicles for space entry are considered. Due to its fast burning rate, as well as, high specific energy content, hydrogen fuel is capable of producing the required thrust at orbital velocities. Hydrogen as the fuel source also provides benefits in the cooling capacity field. As hydrogen is stored at very low temperatures, it can be used as an active cooling fluid on critical temperature parts of the vehicle body. This procedure is generally not possible when considering hydrocarbon fuels. The main disadvantages of hydrogen fuel for scramjet reside on its very low density and lower energy per unit volume compared to hydrocarbon variants. The added weight and mass from the extra fuel has a compounding effect as although there have been significant attempts to develop SSTO vehicles, most still depend on some additional mechanism to achieve the speeds required for the engine to be feasible. The main methods include the incorporation of a low speed engine into the design of the vehicle, or some form of booster rocket or assistance to reach the high speeds.

TABLE 1.1: Basic Properties of Hydrogen and some common Hydrocarbons.

Fuel	Energy/Mass (MJ/kg)	Energy/Volume (MJ/dm^3)	Density (kg/m^3)
Liquid H_2	116.7	8.2	71
Slush H_2	116.6	9.8	82
Methane	50.0	20.8	424
JP-7	43.9	34.7	790
Kerosene	42.8	34.2	800

1.8 Current Scramjet Engine Technology Challenges

Several technical challenges arise in scramjet operation in order to achieve a high efficiency, such as, fuel air mixing, thermal management of engine heat loads and leading edge heat flux amplification, and structures and materials to withstanding the hypersonic flight environment (see Figure 1.13). The scramjet engine represents the center of attention in what concerns to thermal management schemes in hypersonic vehicles due to its potential for extremely high heat loads. It represents a particularly demanding issue due to the sever combustion environment in the flowpath. This environment is characterized by very high thermal, mechanical, and acoustic loading along with hostile, corrosive mix of hot oxygen and combustion products[2]. It can be effectively managed through a combination of structural design, material selection and active cooling.

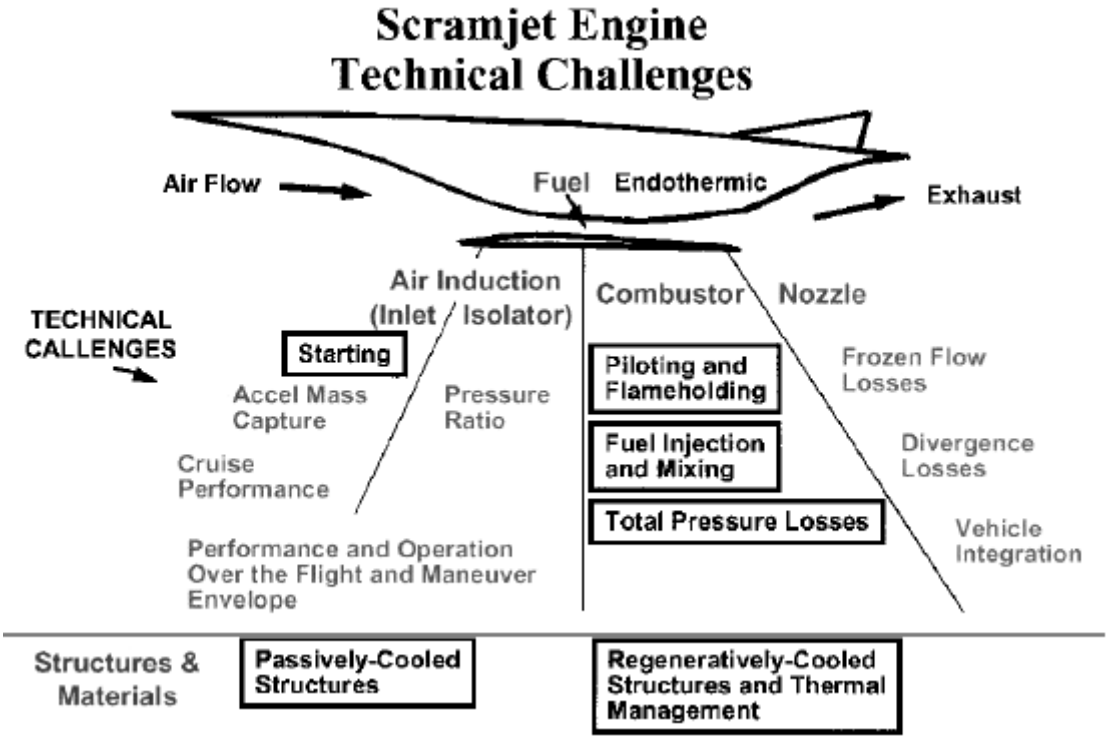

FIGURE 1.13: Technical Challenges of Scramjet Engine Development.
[1]

Beyond the current technical challenges, another area of scramjet development aroused attention. Despite the wide range of possible applications with scramjet technology, the vehicle must first be propelled to a high enough Mach number for the scramjet to start. This requires, depending on the required application, one or two additional propulsion systems to propel the vehicle to the needed scramjet start velocity. Current scramjet designs ambition the start of supersonic combustion to be between Mach 5 and 6. In order to minimize the weight and complexity of having multiple propulsion systems, a dual-mode ramjet/scramjet is often proposed. However, if the necessary scramjet starting Mach number is reduced, a reduction in the number of required additional propulsion systems is attainable, as the gap is bridged between the maximum possible velocity of the low speed engine(s) and the scramjet start velocity. This would result in direct advantages from the outcome reduction in overall vehicle weight, such as, lower mass fraction required for the propulsion system (resulting in more available payload weight), and fewer systems that must work in succession reliably, thereby increasing overall vehicle safety. Hypersonic vehicles also represent an extraordinary challenge for structures and materials, requiring lightweight airframe and engine, as well as high temperature materials and structural configurations that can withstand the severe conditions of the hypersonic flight environment. Typical characteristics of the extreme hypersonic flight environment include[2]:

- Very high temperatures
- Heating of the whole vehicle
- Steady state and transients localize heating from shock waves
- High aerodynamic loads
- High fluctuating pressure loads
- Potential for severe flutter, vibration, fluctuating, and thermally induced stresses.

1.9 Dissertation Layout

This disseration begins with an introduction to the definition of the Scramjet engine. A brief review of the background history development of this kind of engine is also executed. This dissertation is divided in four main parts: Closed Brayton Cycle Thermodynamic Management System analysis (Chapter 2); Optimization Model (Chapter 3); Results and Discussion (Chapter 4) and Conclusions (Chapter 5).
Chapter 2 presents the operating principle as well as a cycle performance model of the Closed Brayton Cycle Thermal Management System.
Chapter 3 presents the description of the optimization model performed, its advantages and how it was implemented.
Chapter 4 presents the results obtained from the optimization and several analysis in order to evaluate the best performance.

Chapter 5 presents the overall conclusions withdrawn from the results obtained as well as future work that can be performed in the scope of the current work.

Chapter 2

Problem Description and Scope of current work

2.1 Working Principle of Closed Brayton Cycle Thermal Management System

The Scramjet thermal management system is a combined balance system, where the heat obtained from direct regenerative cooling of the high temperature wall is totally absorbed by fuel. According to the energy conservation principle, the amount of heat taken away by fuel would be substantially reduced if part of the heat was shifted or discharged to other systems. This would result in a reduction of the fuel flow requirement for cooling. For regeneratively cooled scramjet, the low temperature fuel absorbs as heat, the energy of the high temperature wall through direct cooling. From the second law of thermodynamics, all the available work between the high temperature surfaces and the low temperature fuel heat sink is not maintained and consequently some is wasted. High temperature heat sources made available from the cooling engine and aerodynamically heated surfaces, are potential power suppliers for vehicles operations and potential drivers for subsystems cooling. Hence, if all the available work obtained in heat transfer processes with large temperature difference could be effectively used, it would result in an enhanced performance of the whole energy thermal management system including the regenerative cooling system and fuel cooling capacity (see Figure 2.1).

For hypersonic vehicles there exists several energy requirements, including flight control systems, electronic equipment, fuel supply system, radar communication systems and environmental control systems, etc. The energy recovered between the high temperature surfaces and low temperature fuel could provide power for all these systems. It is possible to establish a closed power generation system if the high temperature wall of the scramjet engine and fuel are regarded, respectively, as high temperature heat source and low-temperature heat source. As mentioned before, part of the heat between the aerodynamically

heated surfaces and engine cooling can be transformed into electrical power and only residual heat is needed to be taken away by fuel.

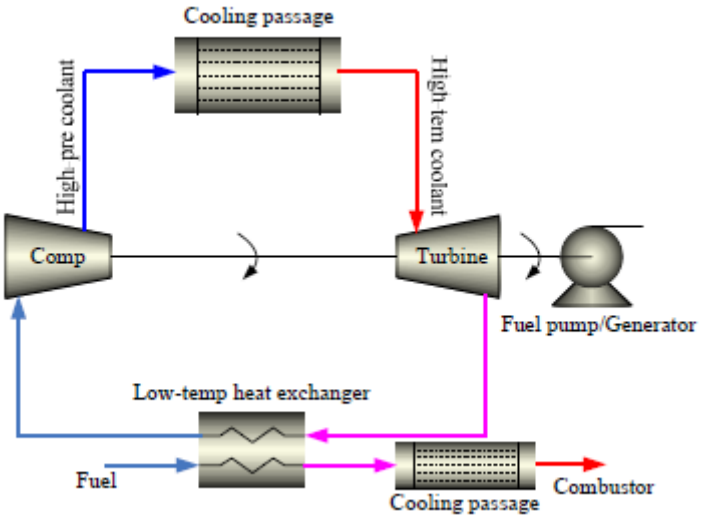

FIGURE 2.1: The Conceptual Thermal Management System of a Scramjet Engine based on Closed Brayton Cycle.
[7]

Initially, coolant for the engine enters into the cooling passage in order to exchange enough heat, and withdraw a large amount of heat generated by aerodynamic heating. This will imply the increase of the gas medium temperature. Thereafter, this high-temperature gas medium enters the turbine where it will expand and produce work which will decrease it's temperature significantly. Next, at the low temperature heat exchanger, the gas medium exchanges heat with the fuel, where the temperature of the gas will reach its lowest point and the fuel temperature rises lightly. Finally, the cooling medium reenters into the cycle after being compressed by the compressor, starting a new cycle. Due to the fact that the temperature of fuel has not reached the maximum temperature allowed, the fuel heat sink did not reach its saturated state, hence, it can be further used as coolant for other cooling passages. Thermal management system presents a good correlation of components and functions with the original system. Due to the multi-function status of the turbine (increase the pressure of gas medium, booster the pressure of fuel and supply electricity for the vehicle), combined with the purpose of the fuel pump, an equivalent to the original power generating system is obtained. Furthermore, the output work of the turbine could drive the compressor, fuel pump and electric generator. Active cooling of aerodynamically heated surfaces at maximum allowable temperatures as well as the scramjet engine cooling could be regarded as sources of additional available work. Closed Brayton Cycle thermodynamic power systems have been successfully applied in space solar thermodynamic power system, nuclear space power system and modular high temperature gas cooled reactor (MHTGR) of nuclear power plant [8].

2.2 Definition of Multiplication Ratio of fuel Heat Sink

To evaluate the performance of CBC Thermal Management System and obtain the performance parameters, it is necessary to compare the performance difference between CBC Thermal Management System and the regenerative cooling system (see Figure 2.2). At the same heating condition, the total cooling process is assumed to be composed by two sections. For regenerative cooling, two high temperature walls are cooled by fuel one after another, all the heat load has to be absorbed by the fuel. For CBC TMS, two high-temperature walls are respectively cooled by helium and fuel. As 'indirect' coolant [8], the heat that fuel has to take away is only the heat discharged by helium at the low-temperature heat exchanger. Fuel could be further used for secondary cooling of $wall_2$, due to the fact that at the exit of low-temperature heat exchanger, fuel does not reach it's saturated heat sink temperature. The same initial parameters and ending temperature of fuel are assumed in order to fully use it's cooling capacity. The pressure drop in the cooling passage is ignored.

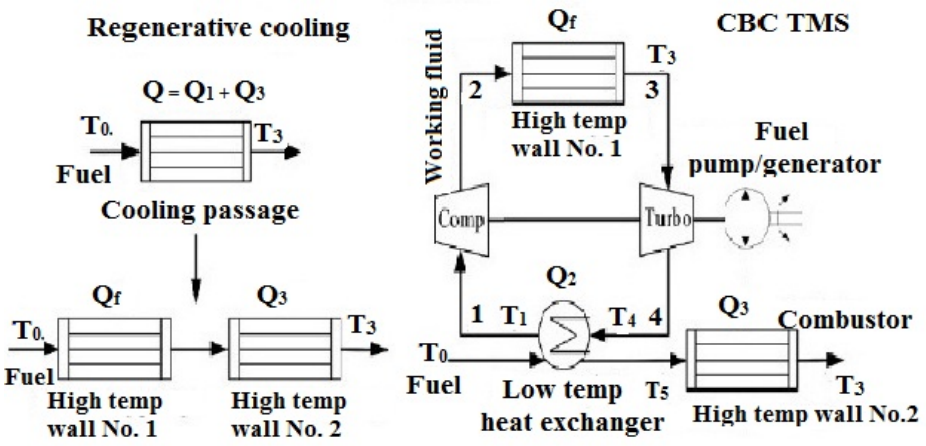

FIGURE 2.2: Comparison Between Regenerative Cooling and CBC TMS. [8]

For regenerative cooling the heat absorbing relation of fuel can be represented as

$$Q_1 = m_1 \times C_p \times (T_3 - T_0) \tag{2.1}$$

For CBC Thermal Management System the heat absorbing relation of fuel can be expressed as

$$Q_2 = m_2 \times C_p \times (T_5 - T_0) \tag{2.2}$$

Fuel relation for the second cooling can be expressed as

$$Q_3 = m_2 \times C_p \times (T_3 - T_5) \tag{2.3}$$

Additionally, Q_1 and Q_2 satisfy the relation

$$Q = Q_1 + Q_3 \tag{2.4}$$

The cycle efficiency, η, of CBC thermal management system can be written as

$$\eta = 1 - \frac{Q_2}{Q_1} = \frac{W}{Q_1} \tag{2.5}$$

Furthermore, the available work of cycle (W) can be represented by

$$W = Q_1 - Q_2 = Q_1 \times \eta \tag{2.6}$$

Q, Q_1, Q_2 and Q_3 represent respectively, the heat transfer of the whole cooling process, $wall_1$, low-temperature heat exchanger and $wall_2$. m_1 and m_2 are, respectively, the fuel flow for regenerative cooling and thermal management system. C_P is the specific heat of fuel at constant pressure for cooling, which is assumed to be constant. T_0, T_3, T_5 represent, respectively, the entrance and exit temperatures of fuel at the cooling passage, and the exit temperature of fuel at the low-temperature heat exchanger. By defining Δm as fuel flow saving ratio,

$$\Delta m = \frac{m_2}{m_1} = 1 - \frac{\eta \times (T_3 - T_0)}{(T_3 - T_0) + (T_3 - T_5) \times (1 - \eta)} > 1 \tag{2.7}$$

Considering cycle efficiency is not equal to zero, the introduction of the CBC thermal management system will reduce the fuel flow for cooling. To assay the degree of 'indirect' enhancement of fuel heat sink, the multiplication ratio of fuel heat sink is defined. For regenerative cooling, fuel cooling capacity can be represented as

$$Q = m_1 \times h_{fc} \tag{2.8}$$

The cooling capacity relation of fuel for closed thermal management system, can be expressed as

$$Q = m_2 \times h'_{fc} \tag{2.9}$$

Where, h_{fc} and h'_{fc} are respectively, the actual and the 'indirect' heat sink. Multiplication ratio of fuel heat sink can be defined as

$$\delta = \frac{h_{fc}^{'} - h_{fc}}{h_{fc}} = \left(\frac{T_5 - T_0}{(T_3 - T_0) \times (\frac{1}{\eta} - 1)}\right) > 0 \tag{2.10}$$

This equation reveals that δ is always greater than zero as long as cycle efficiency is not equal to zero, and will increase as the cycle efficiency increases. Furthermore, δ is only function of cycle efficiency, when the entrance and exit temperatures of the two heat transfer processes are fixed. Therefore, to further evaluate the performance of Closed Brayton Cycle thermal management system, the subsequent analysis will focus on the effect of multiplication ratio of fuel heat sink with cycle characteristic parameters.

2.3 Closed Brayton Cycle Thermal Management System performance model

In order to have the most truthfully performance analysis of the thermal management system, a cycle analysis model considering all sorts of irreversible losses is established. The cooling of the combustor wall will be chosen as the analytical object due to the fact that most of the aeroheating comes from the combustor. Combustion with continuous injection in a scramjet chamber is considered, which maintains the wall combustion chamber at a constant high temperature T_w. Consequently, the heat from the high-temperature heat source can be removed at the constant temperature heat exchanger with infinite heat capacity rate, due to limit resources. A temperature-entropy (T-S) diagram of irreversible Closed Brayton Cycle working between the high-temperature heat source and the low-temperature heat source is shown in Figure 2.3.

1-2-3-4-1 represent the working processes of the cycle, in which, 2-3 is the heat absorbing process from high-temperature heat source, 4-1 is the exothermic heat process to variable-temperature low-temperature heat sink, 1-2 and 3-4 are,respectively, compression and irreversible expansion processes. The cycle working fluid is regarded as an ideal gas, with constant heat capacity rate, C_{wf}, which is the product of mass flow rate and specific heat at constant pressure. T_1, T_{2s}, T_3, T_4 and T_{4s} are the temperatures of the working fluid at state points 1, 2s, 3, 4 and 4s, as for P_1, P_2, P_3, P_4, respectively.

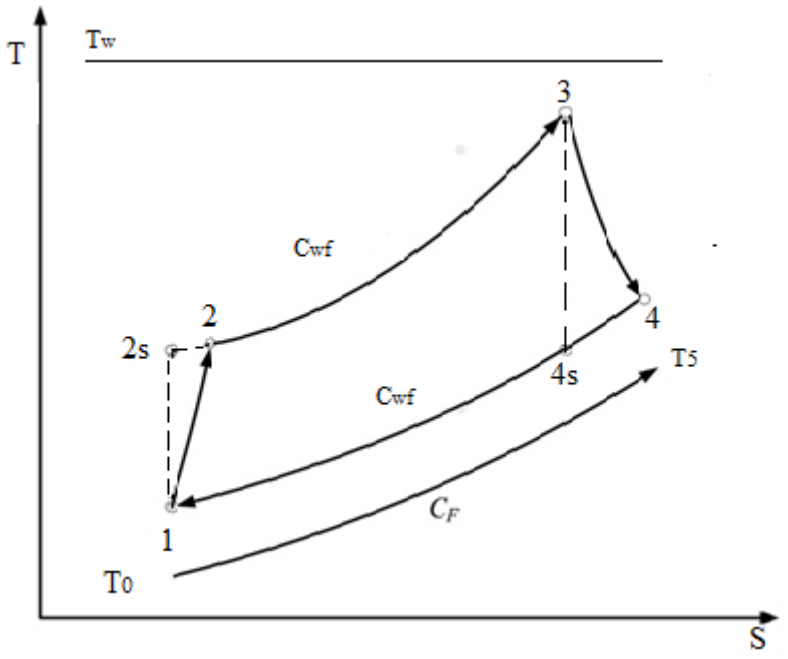

FIGURE 2.3: T-S Diagram of Closed Brayton Cycle with Variable Temperature Low-Temperature Heat Source.
[7]

$\pi = \frac{P_2}{P_1}$ is the compressor pressure ratio. Pressure loss in flow processes is integrated and expressed with a total pressure recovery coefficient $D = \frac{1-\Delta P}{P}$. Therefore,

$$\frac{P_3}{P_4} = \frac{D \times P_2}{P_1} = D \times \pi \tag{2.11}$$

Internal loss of compressor and turbine are defined by the isentropic efficiency, η_c and η_t, with

$$\eta_c = \frac{T_{2s} - T_1}{T_2 - T_1} \tag{2.12}$$

$$\eta_t = \frac{T_3 - T_4}{T_3 - T_{4s}} \tag{2.13}$$

C_H represents the heat capacity rate of high-temperature heat source, while C_F is the heat capacity rate of the low-temperature heat source. High-temperature and low-temperature side heat exchangers are both considered as counterflow heat exchangers. Using the relations for heat transfer between the working fluid and heat source, the nature of working fluid and the theory of heat exchangers, the heat absorbing and heat release rates could be achieved through

$$Q_H = C_{wf} \times (T_3 - T_2) = C_{wf} \times \varepsilon_H \times (T_w - T_2) \tag{2.14}$$

$$Q_L = C_{wf} \times (T_4 - T_1) = C_F \times (T_5 - T_0) = C_{Lmin} \times \varepsilon_L * (T_4 - T_0) \tag{2.15}$$

Where, ε_H and ε_L represent, respectively, the heat exchanger validity of high-temperature and low-temperature side heat exchanger, $C_{Lmin} = min\left\{C_F, C_{wf}\right\}$.

Deducing from Q_L we obtain

$$\frac{C_F}{C_{wf}} = \frac{(T_4 - T_1)}{(T_5 - T_0)} \tag{2.16}$$

This equation reveals that the value of C_{Lmin} is obtained by the ratio of heat transfer temperature difference of both sides of low-temperature heat exchanger. Constant entropy temperature ratio of compressor is defined as $\chi = \pi^m$, where $m = \frac{K-1}{K}$ and K is the adiabatic index.

$$\frac{T_3}{T_4 s} = \frac{(P_3)^m}{(P_4)} = (\pi \times D)^m = \chi \times D^m \tag{2.17}$$

Power output and cycle thermal efficiency can be written as

$$W = Q_f - Q_L \tag{2.18}$$

$$\eta = \frac{W}{Q_f} = 1 - \frac{Q_L}{Q_f} \tag{2.19}$$

Applying the irreversible heat transfer analysis to the Brayton Cycle, cycle thermal efficiency can be expressed as

$$\eta = 1 - \frac{C_{Lmin} \times \varepsilon_L \times [d \times \varepsilon_H \times \tau - \eta_c + d \times f \times (1 - \varepsilon_H)]}{\varepsilon_H \times [(\eta_c \times C_{wf} - c \times d * f) \times \tau - f \times C_{Lmin} \times \varepsilon_H]} \tag{2.20}$$

The dimensionless power is defined as $\overline{W} = \frac{W}{C_{wf} * T_{Lin}}$ so one can define

$$\overline{W} = \frac{[\eta_c \times \times C_{wf} - d \times (c \times f + \eta_c \times C_{Lmin} \times \varepsilon_H)] \times \varepsilon_H \times \tau - [f \times (d \times (1 - \varepsilon_H) + \varepsilon_H) \times C_{Lmin} \times \varepsilon_H]}{(\eta_c \times C_{wf} - c \times d \times f) \times (1 - \varepsilon_H)} \tag{2.21}$$

Where,$c = C_{wf} - C_{Lmin} \times \varepsilon_L$, $d = 1 - \eta_t + D^{-m} * \chi^{-1} * \eta_t$, $f = \chi - 1 + \eta_c$, $\tau = \frac{T_w}{T_0}$ are temperature ratio between high-temperature and low-temperature heat source. Multiplication ratio of fuel heat sink can be further expressed from Eq.(2.11) and Eq.(2.20) as

$$\delta = \frac{(T_5 - T_0) \times [\varepsilon_H \times [(\eta_c \times C_{wf} - c \times d \times f) \times \tau - f \times C_{Lmin} \times \varepsilon_L] - C_{Lmin} \times \varepsilon_L \times d \times \varepsilon_H \times \eta_c \times \tau - \eta_c + d \times f \times (1 - \varepsilon_H)]}{(T_3 - T_0) \times C_{Lmin} \times \varepsilon_L \times [d \times \varepsilon_H \times \eta_c \times \tau - \eta_c + d \times f \times (1 - \varepsilon_H)]} \tag{2.22}$$

Furthermore, from Eq.(2.15) and considering the fact that T_0 and T_1 are usually fixed parameters, T_4 and T_5 are the key parameters to determine C_{Lmin}. More specifically T_5 will determine the heat absorption distribution of fuel between the low temperature heat exchanger and the second high temperature wall, and also determines the relationship between working fluid heat capacity rate and fuel capacity rate. In order to reduce the fuel flow rate for cooling the fuel heat capacity rate C_F should be as small as possible. High values of T_5 should be chosen to make $C_F < C_{wf}$, therefore $C_{Lmin} = C_F$. Thus T_5 can be determined as

$$T_5 = \varepsilon_L \times T_4 + (1 - \varepsilon_L) \times T_0 \tag{2.23}$$

Chapter 3

Optimization Model

To obtain the maximum performance it is necessary to build a cycle optimization model. An optimization problem generally consists of an objective function $F(X_1, X_2, \ldots, X_n)$ to be minimized for design variables X_i for $i = 1, 2, ..., n$. The design variables may have lower or upper bounds (side constraints). The multiplication ratio of fuel heat sink (δ) is chosen as the optimization objective index. The design variables are T_0,T_1, T_w, ε_f, ε_l, η_c, η_t, D, π and C_{Lmin}. The lower and upper limits for design variables are determined by cycle constraints.

3.1 Definitions

Considering D a compact subset of $\Re^n$ and f:D $\rightarrow \Re$ a function. One point $x^* \in$ D is a local minimizer of f in D if exists a neighborhood V of x^*, with $V \subseteq D$, such as[9]:

$$\forall x = (x_1, \ldots, x_n) \in V, f(x^*) \leq f(x) \tag{3.1}$$

In this case the number, $y^* = f(x^*)$ is a local minimizer of f in D. A function can have several local minimizers with the correspondents local minimums being eventually different from each other. The point $x^* \in D$ is a global minimizer of f in D if[9]:

$$\forall x = f(x^*) \leq f(x) \tag{3.2}$$

In this case $y^* = f(x^*)$ is a global minimum of f in D. Although a function can have several global minimizers, it has only one global minimum, i.e., if there exists several global minimizers $x_1^*, x_2^*, ..., x_p^*$, so:

$$f(x_1^*) = f(x_2^*) = \ldots = f(x_p^*) \tag{3.3}$$

Proposition 1[9]: Any global minimizer of *f*: D $\rightarrow \Re$ is as well a local minimizer of *f* in D, but there are local minimizers that are not global minimizers of *f*.

Corollary 1[9]: If *f*: D $\rightarrow \Re$ only has one local minimizer, this minimizer is the global minimizer of *f* in D.

Definition 2[9]: Minimizing a function *f* on a D domain means searching for at least one minimizer (local or global) of *f* in D and the correspondent minimum (local or global). By stipulation, is written $min_{x \in D} f(x)$, to say: minimizing f in D, or: $max_{x \in D} f(x)$, to say: maximize *f* in D.

Proposition 2[9]: Maximize *f* in D is equivalent to minimizing (-*f*) in D. This proposition means that the maximizers of a function *f* in D are the minimizers of the opposite function (-*f*) in D.

3.2 Gradient Method

The gradient of a function *f* in $x \in \Re^n$ is the vector defined by[9]:

$$\nabla f(x) = \left[\frac{\partial f(x)}{\partial x_1}, \frac{\partial f(x)}{\partial x_2}, \ldots, \frac{\partial f(x)}{\partial x_n} \right]^T \tag{3.4}$$

The gradient of a multivariable function in a determined x point is the maximum direction of ascent when it moves from the point x on the curve of this function. A displacement from the point x over this curve and in the direction $\nabla f(x)$ results in a bigger ascent over any other direction with a course of the same length. For the same reason, a course in the opposite direction to the gradient results in a maximum descent. This way, it is clear that following each time the opposite direction on the course over the function curve, sooner or later, a minimum will be found. The gradient method is an iterative method of searching that starts from an initial point $x_0 \in D$ (generally chosen arbitrarily), that will define the vector x_{k+1} from the x_k formula:

$$x_{k+1} = x_k + \lambda_k * d_k \tag{3.5}$$

Where $\lambda_k \in \Re$ and d_k is a vector that indicates the direction of descent to reach a minimum of the function *f*. This means that we must have:$(\nabla f(x))_k^T * d_k \leq 0$ to ensure the descent. The basic case is when is considered $d_k = -\nabla f(x_k)$. The iterations finish when $\|dk\|$ reaches a value relatively close to zero. To chose the best descent step, λ_k, to ensure the convergence to a minimum of *f* the methods of choice are:

1. In the gradient method with bigger descent, it is chosen λ_k equal to the value of $\lambda \geq 0$ that minimizes the function g defined by any λ:

$$g(\lambda) = f(x_k + \lambda d_k) \tag{3.6}$$

2. Instead of finding the optimum value of λ_k has it is done in the gradient case with bigger slope, can only chose λ_k equal to a value $\lambda \geq 0$ so that:

$$f(x_k + \lambda d_k) = f(x_k) \tag{3.7}$$

3. Or the parameter λ_k can be chosen so that the sequence $(\lambda_k)_{k\geq 0}$ converge to zero and that $\sum_{k=0}^{+\infty} \lambda_k = +\infty$.

In order to solve a constrained optimization problem is necessary to transform it in an unconstrained optimization problem through an exterior penalty function:

$$\phi(x,\mu) = f(x) + \mu \times [\sum_{i=1}^{m} (Max[0, g_i(x)])^2 + \sum_{i=1}^{p} (h_i(x))^2] \tag{3.8}$$

where μ is a large positive number, corresponding to the penalty number. When an inequality constraint is satisfied, then $g_i < 0$ and $Max[0, g_i]$ will return 0 and therefore there will be no contribution of the function ϕ. If a constraint is violated, i.e. $g_i > 0$ or $h_i \neq 0$, a large term will get added to ϕ. Minimizing ϕ should eliminate the violation. In order to achieve results with this method the penalty number, μ, should be very large. In fact, theoretically, the minimum of ϕ corresponds to the solution of the original problem as $\mu \to \infty$.

One of the advantages of the gradient method and of its variants is that they converge quickly. However this method requires the derivability of the function to be minimized and the calculus of the gradient (compound by the partial derivates) of this function in each iteration. The gradient method is recommended for the following conditions[9]:

1. The dimension of the problem (i.e., the number of monodimensional variables of the problem) is relatively small.
2. The expression of the function f is not very complex, i.e, the evaluation of f is not very long.
3. The function f is derivable and the partial derivates can be calculated easily.
4. Seeks to find only one local minimizer of the function f.

3.2.1 General Algorithm Description

The function *fmincon* in the MATLAB Optimization Toolbox attempts to find the minimum of a constrained nonlinear multivariable function starting at an initial estimate.

$$min_x f(x)$$

subject to

$c(x) \leq 0$
$ceq(x) = 0$
$A.x \leq b$
$Aeq.x = beq$
$lb \leq x \leq ub$

where x, b, beq, lb, and ub are vectors, A and Aeq are matrices, $c(x)$ and $ceq(x)$ are functions that return vectors, and $f(x)$ is a function that returns a scalar. $f(x)$, $c(x)$, and $ceq(x)$ can be nonlinear functions. The function that computes the nonlinear inequality constraints is $c(x) \leq 0$ and the nonlinear equality constraints is $ceq(x) = 0$. The actual optimization is performed iteratively.

A general step by step description of the optimization process algorithm is given below:

1. Define the objective function to be minimized ($f(x)$).
2. Define the non linear constraints of the objective function.
3. Start at an initial estimated value $x_0 \in \Re$.
4. Invoke the constrained optimization routine.

3.2.2 Limitations

The performance of a gradient based method strongly depends on the initial values chosen. Several optimization runs with different initial values might be necessary if no a priori knowledge (e.g., the result of a process simulation) about the function to optimize can be applied.
The function to be minimized and the constraints must both be differentiable. *fmincon* may only give local solutions.
The objective function and constraint function must be real-valued, that is, they cannot return complex values.

Chapter 4

Results and Analysis

A numerical computing environment, MATLAB, was used to build an optimization algorithm to provide comprehensive numerical examples in order to evaluate the heat exchanger effectiveness, as well as, the turbine and compressor effectiveness, the pressure recovery coefficients, the cycle pressure ratio and the influence of T_5 in the parameters; multiplication ratio of fuel heat sink (δ), efficiency (η_{th}), and dimensionless power ($\overline{W}$). To obtain a numerical appreciation of the results, several parameters were considered: effectiveness of the various heat exchangers (ε_H and ε_L) in the range of 0.70-1.00, turbine and compressor efficiencies (η_t and η_c) in the range of 0.85-1.00, total pressure recovery coefficient (D) between 0.88-1.00 and cycle pressure ratio (π) between 1.5-25, with $C_{wf} = 1.0$ kW/K, $\gamma = 1.67$, $T_w = 1000$ K, $T_0 = 25$ K and $T_1 = 150$ K. The effect of each parameters was analyzed (while keeping the others constant) on the various temperatures state points, heat transfer rates, thermal efficiency, multiplication ratio of fuel heat sink and power output.

4.1 Effect of various effectivenesses

4.1.1 Variation of multiplication ratio of fuel heat sink with heat exchanger effectiveness and cycle pressure ratio

Figure 4.1, illustrates the variation of the multiplication ratio of fuel heat sink with the effectivenesses of first cooling (ε_H) and low temperature heat exchanger (ε_L). δ increases with the increase of the effectivenesses, and higher values of these heat exchangers effectivenesses decrease the external irreversibilities on their respective sides by forcing the working fluid or fuel to transfer heat to and from the sink/sources by increasing the heat transfer rates and decreasing the temperature differences. Ideal heat exchanger effectivenesses when compared with real heat exchanger effectiveness, represent the most efficient Brayton cycle, however, no ideal heat exchanger is available in practice. Hence, heat transfer losses are crucial to conclude any results in the analysis of the Brayton cycle. It is very important to consider irreversible loss in heat transfer process for CBC TMS performance analysis. Multiplication ratio of fuel heat sink variation along the increase of π presents a curve, and there exists an optimal π for each curve to make δ obtain its maximum value. This variation can be explained by two processes. In one hand, the thermal efficiency presents a similar variation, and it has a strong effect on the multiplication ratio of fuel heat sink. On the other hand, T_4 decreases as the increase in cycle pressure ratio (π), and the fuel temperatures at low temperature heat exchanger (T_5) and second cooling passage will correspondingly decrease. The decrease of T_5 indicates that the amount of fuel needed to be removed by fuel gradually decreases, which favors the reducing of fuel flow for cooling. However, the decrease of T_5 also implies the decrease of the temperature in the second cooling passage which will make the heat absorption of fuel decrease, consequently increasing the fuel flow for cooling.

Before reaching the optimal π, the gain of reducing the fuel flow for cooling in low temperature heat exchanger is prominent, and δ gradually increases and obtains its maximum value at optimal π. After the optimal π, due to the decrease of heat absorption of fuel in the second cooling passage, fuel flow for cooling becomes dominant and increases with π, making δ decrease. The case that δ is negative is possible and illustrates that the presented CBC TMS does not bring any benefit when compared with conventional regenerative cooling but additional irreversible loss in the low temperature heat exchanger and compressor. Hence, choosing a correct and proper value of cycle pressure ratio is of crucial importance to achieve a good performance. Furthermore, the optimal cycle pressure ratio for δ is achieved at relatively small values, and it is smaller than the optimal cycle pressure ratio for thermal efficiency. Resuming, relatively good performance for CBC TMS for a small π is favorable for actual design and operation.

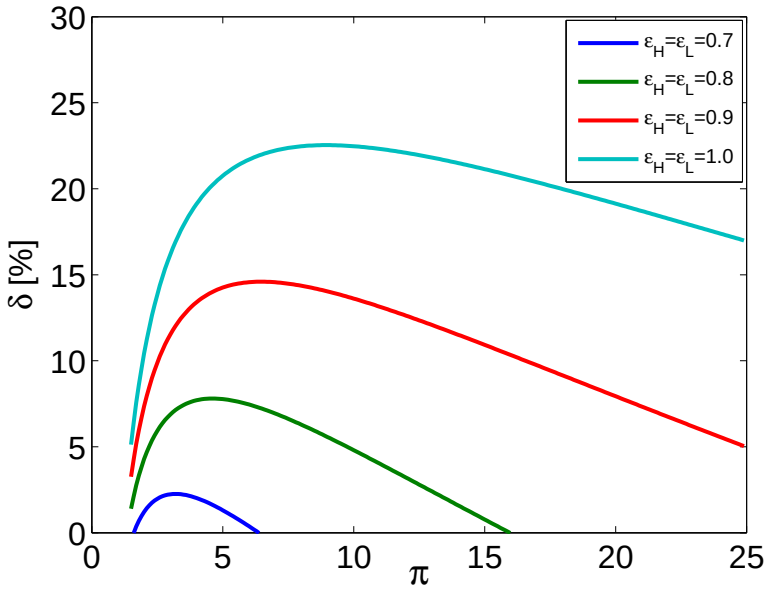

FIGURE 4.1: Effect of Heat Exchanger Efficiency and Cycle Pressure Ratio on Multiplication ratio of Fuel Heat Sink, when
$\eta_c = \eta_t = 0.85$ and $D = 0.93$.

4.1.2 Variation of thermal efficiency with heat exchanger effectiveness and cycle pressure ratio

The variation of thermal efficiency (η_{th}) with cycle pressure ratio and heat exchanger effectiveness is illustrated in Figure 4.2. There is also an optimal π for each curve. Furthermore, thermal efficiency increases as the effectivenesses increases. Differences among thermal efficiencies at different heat exchanger effectivenesses are relatively small for low cycle pressure ratios, however, as cycle pressure increases, these differences become gradually substantial.

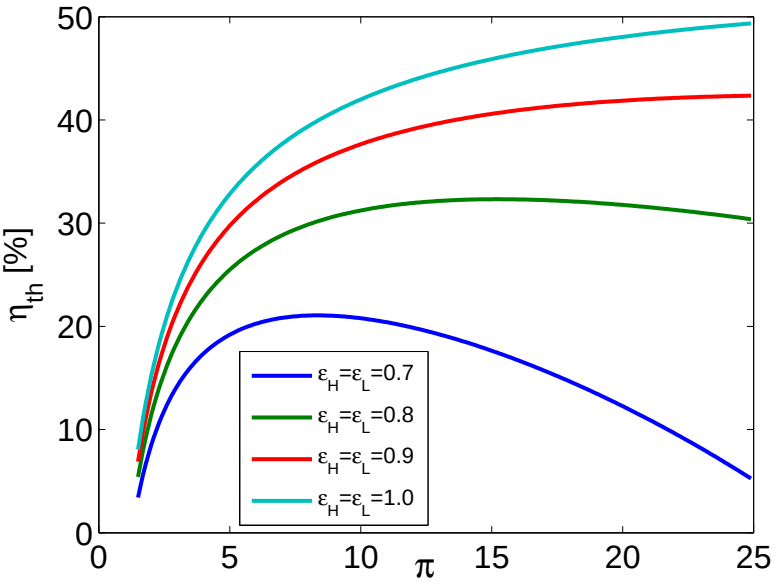

FIGURE 4.2: Effect of Heat Exchanger Efficiency and Cycle Pressure Ratio on Thermal Efficiency, when
$\eta_c = \eta_t = 0.85$ and $D = 0.93$.

4.1.3 Variation of dimensionless power with heat exchanger effectiveness and cycle pressure ratio

Dimensionless power variation with heat exchanger effectivenesses and cycle pressure ratio has similar results (see Figure 4.3) with that on δ. Network output is the byproduct of CBC TMS. Work output can be regarded as the power source for the fuel feeding subsystem and power generation subsystem. This conclusion has a particular promising application in aerospace planes and fully reusable space transport vehicles future. From the analysis previously addressed, the optimal performances of the CBC TMS can be obtained through reducing the irreversibility of the components, and choosing the proper matching between the thermal capacitance rate of working fluid and the reservoirs.

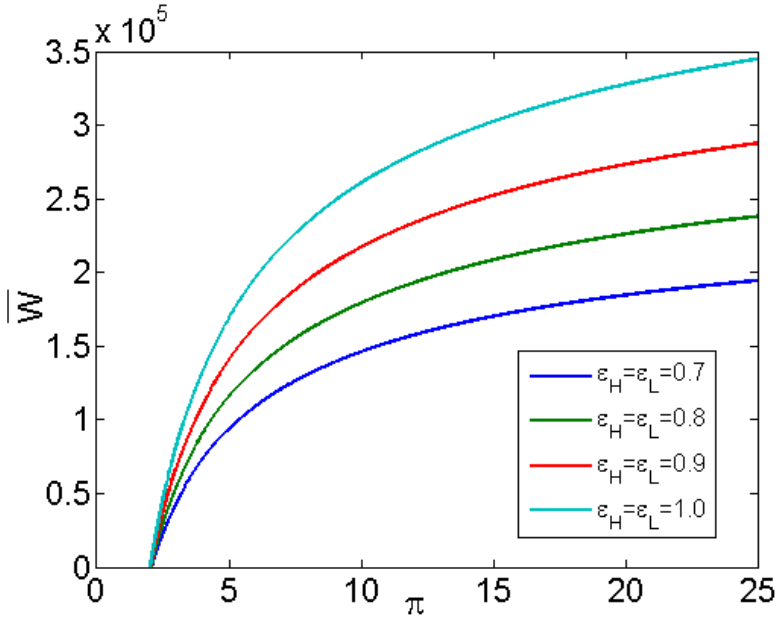

FIGURE 4.3: Effect of Heat Exchanger Efficiency and Cycle Pressure Ratio on Specific Net Work Output

4.2 Effect of compressor and turbine efficiencies

Figure 4.4 illustrates the variation of multiplication ratio of fuel heat sink with the increase of both efficiencies. High performance compressor and turbine is critical to obtain good performance for the CBC TMS. Furthermore, there is no optimal cycle pressure ratio when $\eta_c = \eta_t = 1.0$, which further shows the importance of the consideration of various irreversible losses.

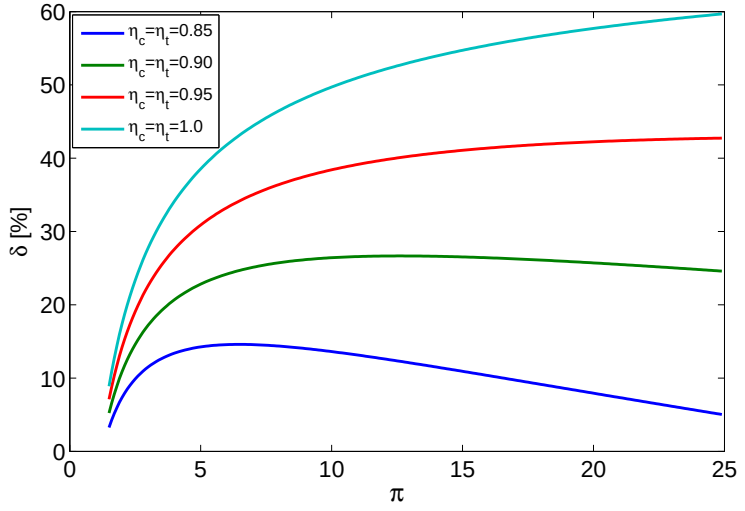

FIGURE 4.4: Effect of Turbine and Compressor Efficiencies on Multiplication ratio of Fuel Heat Sink, when
$\varepsilon_H = \varepsilon_L = 0.9$ and $D = 0.93$.

4.3 Effect of pressure loss

As shown in Figure 4.5, δ increases as the pressure recovery coefficients decrease, i.e., as the decrease of pressure loss. Variation of δ with the pressure recovery coefficients is similar to that of heat exchanger. Hence, how to reduce the pressure loss is also crucial for achieving a better CBC TMS performance.

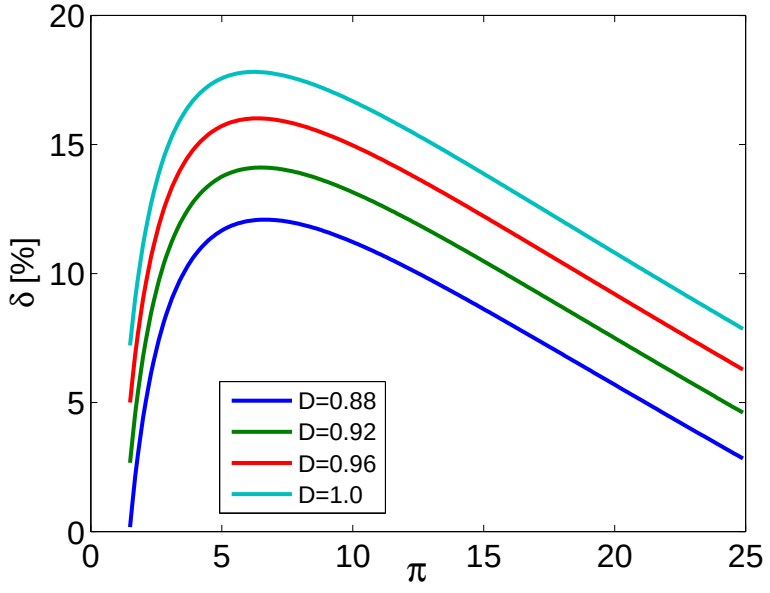

FIGURE 4.5: Effect of Pressure Loss on Multiplication ratio of Fuel Heat Sink, when
$\varepsilon_H = \varepsilon_L = 0.9$ and $\eta_c = \eta_t = 0.85$.

Chapter 5

Conclusions

The present work led to important conclusions about the performance of a Closed Brayton Cycle Thermal Management System (CBC TMS) for a scramjet engine. Through cycle analysis the results show that CBC TMS presents a great potential, not only on the reduction of fuel flow for cooling but also on providing available work for the whole vehicle. The multiplication ratio of fuel heat sink is defined as a performance parameter to evaluate the CBC TMS performance comparatively with regenerative cooling. Significant improvements over the conventional regenerative cooling were achieved, with multiplication ratio of fuel heat sink as high as 51% and additional work output for the whole vehicle. Its benefits can be addressed as follows. Initially, as fuel is not directly used as coolant, fuel demand for cooling is reduced and consequently, fuel heat sink is increased. Thermal protection system difficulties are mitigated, and engine size and weight are probably reduced, improving scramjet engine as well as overall hypersonic vehicle performance. Furthermore, the available work between high temperature wall and low-temperature fuel is recuperated, enabling the supply of energy to electric generation system, fuel supply system and other vehicle subsystems. Ultimately, using inert fluid as coolant improves reliability and security, notably for manned hypersonic vehicles. The effects of several parameters on CBC TMS performance have been considered. High effectivenesses of the various heat exchangers, high efficiencies of turbine and compressor, as well as, high total pressure recovery efficient are favorable to obtain a good performance. Heat capacitance rates also play an important role in determining the CBC TMS performance, and it is found that there is a required order in choosing the heat capacitance rates of the fuel and the working fluid. For this case, the order is found to be $C_{wf} \geq C_F$. Furthermore, the maximum value of multiplication ratio of fuel heat sink will be obtained at the optimal cycle pressure ratio π, and π is relatively small, which is favorable for CBC TMS realization.

5.1 Future Recommendations and Goals

Promising advances have been made in the high-speed airbreathing propulsion field. There are a number of future potential missions and applications for hypersonic vehicles powered by high-speed propulsion

systems. Closed Brayton Cycle Thermal Management System holds significant promise for extending the flight Mach number envelope of conventional hypersonic airbreathing engines. Future work should continue to develop and improve propulsion systems and efforts should be made on vehicle classes that will allure the interest of potential users. Vehicles of interest include hypersonic cruise vehicles, reconnaissance and return, hybrid rocket-scramjet systems where the scramjet is used as an enhancer of specific impulse[10].
Proper directions and technologies development required to improve vehicle and propulsion systems, should primarily focus on[10]:

- Scramjet technology.
- Hypervelocity propulsion (including shock initiated combustion, detonation and pulse detonation engines).
- Hydrogen and hydrocarbon ramjet technology.
- Revolutionary propulsion systems.
- Fuels technology.
- Engine/airframe integration.
- Performance analysis techniques (both cycle and CFD).
- Engine controls (isolator-combustor-fuel feedback systems).
- Flowfield diagnostics.
- Ground-based propulsion simulation techniques (with emphasis on hypervelocity).

Appendix A

Appendix

TABLE A.1: Worldwide Scramjet Evolution, 1955-1990

Era	Country/service	Engine/vehicle	Engine type	Dates, year	Cruise Mach no.	Cruise altitude, ft	Powered range, n mile	Launcher	Total length, in.	Diameter, in.	Total weight, lbm	State of development
1955–1975	U.S. Navy	External burn[b]	ERJ	1957–1962	5–7	—	—	—	—	—	—	Combustion tests
	Russia	Chetinkov research	ERJ	1957–1960	5–7	—	—	—	—	—	—	Component tests
	U.S. Air Force	Marquardt SJ	DMSJ	1960–1970	3–5	—	—	—	88	10 x 15	—	Cooled engine tests
	U.S. Air Force	GASL SJ[a]	SJ	1961–1968	3–12	—	—	—	40	31 in^2	—	Cooled engine tests
	U.S. Navy	SCRAM[b]	LFSJ	1962–1977	7.5	100,000	350	Rail	268	26.2	5,470	Free-jet test
	U.S. Air Force	IFTV[c]	H_2/SJ	1965–1967	5–6	56,000	—	—	—	—	—	Component tests
	U.S. Air Force–NASA	HRE[b]	H_2/SJ	1966–1974	4–7	—	—	—	87	18	—	Flowpath tests
	NASA	AIM[b]	H_2/SJ	1970–1984	4–7	—	—	—	87	18	—	Cooled engine tests
	France	ESOPE[b]	DMSJ	1973–1974	5–7	—	—	—	87	18	—	Component tests
1975–1990	U.S. Navy	WADM/HyWADM[b]	DCR	1977–1986	4–6	80,000–100,000	500–900	VLS	256	21	3,750	Component tests
	Russia	Various research	SJ/DCR	1980–1991	5–7	80,000–100,000	—	—	—	—	—	Combustion tests
	NASA	NASP[b]	MCSJ	1986–1994	0–26	0–orbit	Orbital	Runway	—	—	500,000	Free-jet test (M7)
	Germany	Sänger II[b]	ATRJ	1988–1994	4	0–orbit	Orbital	Runway	3976	550	800,000	Concept vehicle

[3]

TABLE A.2: Worldwide Scramjet Evolution, 1990-2004

Era	Country/service	Engine/vehicle	Engine type	Dates, year	Cruise Mach no.	Cruise altitude, ft	Powered range, n mile	Launcher	Total length, in.	Diameter, in.	Total weight, lbm	State of development
1990–2003	United Kingdom	HOTOL[c]	SJ	1990–1994	2–8	——	——	——	——	——	——	Combustion tests
	Japan	PATRES/ATREX[b]	TRBCC	1990–	0–12	100,000	——	——	87	30	——	Component tests
	Japan	NAL-KPL research[b]	SJ	1991–	4–12	50,000–100,000	——	——	83	8 × 10	——	Component tests
	Russia	Khold[a]	DCR	1991–1998	3.5–5.4	50,000–115,000	——	SA-5	36	24	——	Flight tests
	Russia/France	Khold[a]	DCR	1991–1995	3.5–5.4	50,000–115,000	——	SA-5	36	24	——	Flight tests
	Russia/United States	Khold[a]	DCR	1994–1998	3.5–7	50,000–115,000	——	SA-5	36	24	——	Flight tests
	France	CHAMOS[b]	SJ	1992–2000	6.5	——	——	——	——	8 × 10	——	Component tests
	France	Monomat	DMSJ	1992–2000	4–7.5	——	——	——	——	4 × 4	——	Component tests
	France	PREPA[a]	DMSJ	1992–1999	2–12	0–130,000	Orbital	Ground	2560	Waverider	1×10^6	Component tests
	Russia	ORYOL/MIKAKS	SJ	1993–	0–12	0–130,000	Orbital	Ground	——	——	——	Component tests
	France/Russia	WRR[b]	DMSJ	1993–	3–12	0–130,000	——	Ground	——	Waverider	60,000	Component tests
	Russia	GELA Phase II[a]	RJ/SJ	1995–	3–5+	295,000	——	Tu-22M	——	——	——	Flight tests
	Russia	AJAX[b]	SJ	1995–	0–12	0–130,000	——	——	——	——	——	Concept
	U.S. Air Force	HyTech[a]	SJ	1995–	7–10	50,000–130,000	——	——	87	9 × 12	——	Component tests
	United States	GTX[d]	RBCC[e]	1995–	0–14	50,000–130,000	——	——	——	——	——	Component tests
	U.S. Navy	Counterforce	DCR	1995–	4–8	80,000–100,000	——	Air/VLS	256	21	3,750	Component tests
	NASA	X-43A/Hyper-X[a]	H2/SJ	1995–	7–10	100,000	200	Pegasus	148	60(span)	3,000	Flight tests
	France/Germany	JAPHAR[a]	DMSJ	1997–2002	5–7.6	80,000	——	——	90	4 × 4	——	Component tests
	United States	ARRMD[b]	DCR	1997–2001	3–8	80,000	450–800	Rail/Air	168–256	21	2,200–3,770	Component tests
	Russia	IGLA[a]	SJ	1999–	5–14	82,000–164,000	——	SS-25	197	——	——	Flight tests
	NASA	X-43C[b]	DMSJ	1999–	5–7	100,000	——	Pegasus	——	10.5 wide	——	Component tests
	Unites States	HPTET[b]	ATR	1999–	0–5	0–90,000	——	——	——	15–40	——	Component tests
	United States	RTA[b]	TBCC	1999–	0–5	0–90,000	——	——	——	15–40	——	Component tests
	France	Promethee[b]	DMSJ	1999–2002	2–8	0–130,000	——	——	238	——	3,400	Component tests
	India	AVATAR-M[b]	SJ	1999–	0–14	0-orbit	Orbital	Ground	——	——	18–25 ton	Combustion tests
	United Kingdom	HOTOL Phase II	SJ	2000–	2–8	——	——	——	——	——	——	Component tests
	France	PIAP[b]	DMSJ	2000–	2–8	0–110,000	——	——	53	8 × 2	——	Component tests
	United States	MARIAH	MHD/SJ	2001–	15	——	——	——	——	——	——	Combustion tests
	Australia	HyShot[b]	SJ	2001–2002	7.6	75,000–120,000	200	Terrior Orion	55	14	——	Flight tests
	United States	Gun launch technology	SJ	2001–	——	——	——	Ground	——	——	——	Flight tests
	United States	ISTAR[b]	RBCC[e]	2002–2003	2.4–7	0-orbit	Orbital	Ground	400	Waverider	20,000	Component tests
	United States	X-43B[b]	RB/TBCC	2002–2003	0–10	100,000	200	Air	500	Waverider	24,000	Component tests
	Russia	Mig-31 HFL[b]	SJ/DCR	2002–	2–10	50,000–130,000	——	Mig–31	——	——	——	Planned flight tests
	United States	HyFly[a]	DCR	2002–	3–6.5	85,000–95000	600	F-4	225	19	2,360	Flight tests planned
	United States	SED[a]	SJ	2003–	4.5–7	80,000	——	——	——	9 wide	——	Planned flight tests
	France	LEA[a]	SJ/DCR	2003–2012	4–8	80,000	——	Air	——	——	——	Flight tests planned
	United States	RCCFD[b]	TBCC	2003–	0.7–7	0-orbit	Orbital	Ground	400	Waverider	20,000	Flight tests planned

[3]

Bibliography

[1] K. N. Roberts. Analysis and Design of a Hypersonic Scramjet Engine with a starting Mach number of 4.00. MSc, 2008.

[2] D. Andrealis. Scramjet Engines enabling the seamless integration of air & Space operations. Pratt & Whitney Space Propulsion, West Palm Beach, FL.

[3] R.S. Fry. A Century of Ramjet Propulsion Technology Evolution. *Journal of Propulsion and Power*, 20(1), January-February,2004.

[4] C.E. Cockrell Jr., R.W. Guy, C.R. McClinton, and S.S. Welch. Technology Roadmap for Dual-Mode Scramjet Propulsion to Support Space-Access Vision Vehilce Development. *American Institute of Aeronautics and Astronautics*, NASA Langley Research Center, Hampton, Virginia, USA, 2002.

[5] Adrian Mann. Url: http://www.aerospaceweb.org/design/waverider/examples.shtml. Accessed May,2010.

[6] C.R. McClinton. High speed/hypersonic aircraft propulsion technology development. *Advances on Propulsion Technology for High-Speed Aircraft*, pages 1–32, Neuilly-sur-Seine, France, 2008.

[7] J. Qin, W. Zhou, W. Bao, and D. Yu. Thermodynamic analysis and parametric study of a closed Brayton cycle thermal management system for scramjet. *International Journal of Hydrogen Energy*, School of Energy Science and Engineering, Harbin Institute of Technology, China, 2010.

[8] J. Qin, W. Bao, W. Zhou, and D. Yu. Thermal Management System Performance Analysis of Hypersonic Vehicle Based on Closed Brayton Cycle. *American Institute of Aeronautics and Astronautics*, pages 356–364, Harbin Institute of Technology, China, 2008.

[9] K. Bousson. Optimization by Gradient Methods. *Master's Degree Lecture Notes on Flight Control Systems (in portuguese)*, Department of Aerospace Sciences,University of Beira Interior, Covilhã, Portugal, 2008.

[10] G.L. Pellet, J.P. Drummond, C.E. Cockrell, and *et al*. Hypersonic Airbreathing Propulsion - An Aerodynamics, Aerothermodynamics, and Acoustics Competency White Paper. Langley Research Center,Hampton,Virgina,November, 2002.

[11] K.C. Markell. Exergy Methods for the Generic Analysis and Optimization of Hypersonic Vehicles Concepts. MSc, 2005.

[12] M.J. Lewis. Significance of fuel selection for hypersonic vehicle range. *Journal of Propulsion and Power*, 17(6):1214–1221, January, 2001.

[13] O.A. Powell, J.T. Edwards, R.B. Norris, K.E. Numbers, and J.A. Pearce. Development of hydrocarbon-fueled scramjet engines:the hypersonic technology (hytech) program. *Journal of Propulsion and Power*, 17(6), U.S Air Force Research Laboratory and Universal Technology Corporation, Ohio, November-December, 2001.

[14] L. Chen, W. Wang, F. Sun, and C. Yu. Closed intercooled regenerator brayton-cycle with constant-temperature heat-reservoirs. *Applied Energy*, pages 429–446, Naval University of Engineering and Mechanical Engineering Department, China and USA, July, 2003.

[15] J. Qin, W. Zhou, W. Bao, and D. Yu. Performance limit analysis of recooled cycle for regenerative coooling systems. *Energy Conservation and Management*, pages 1908–1914, School of Energy Science and Engineering, Harbin Institute of Technology, China, 2009.

[16] J. Qin, W. Zhou, W. Bao, and D. Yu. Thermodynamic optimization for a Scramjet with Re-cooled Cycle. *Acta Astronautica*, School of Energy Science and Engineering,Harbin Institute of Technology, China, 2009,(to appear).

[17] S. Leyffer and A. Mahajan. Nonlinear Constrained Optimization: Methods and Software. March 17, 2010.

[18] R.P. Mikkilineni and T. Feagin. A computational method for minimization with nonlinear constraints. *Journal of Optimization Theory and Applications*, 25(3), The University of Tenesse Space Institute, Tenesse, United States of America, July, 1978.

[19] K. Bousson and S.D. Correia. Optimization Algorithm Based on Densification and Dynamic Canonical Descent. *Journal of Computational and Applied Mathematics*, 191:269–279, ISSN: 0377-0427, 2008.

[20] P.J. Waltrup, M.E. White, F. Zarlingo, and E.S. Gravlin. History of U.S. Navy ramjet, scramjet, and mixed-cycle propulsion development. *American Institute of Aeronautics and Astronautics*, John Hopkins University and U.S Navy, Naval Air Warfare Center, 1996.

[21] P.J. Waltrup. Upper bounds on the flight speed of hydrocarbon-fueled scramjet-powered vehicles. *Journal of Propulsion and Power*, 17(6):1199–1204, 2001.

[22] E.T. Curran. Scramjet engines: The first forty years. *Journal of Propulsion and Power*, 17(6):1138–1148, 2001.

[23] M.R. Tetlow and C.J. Doolan. Comparison of hydrogen and hydrocarbon-fuelled scramjet engines for orbital insertion. *Journal of Spacecraft and Rockets*, 44(2):365–373, 2007.

[24] C. Segal. Propulsion Systems for Hypersonic Flight. University of Florida,Gainesville, Fl, 32611, US, 2007.

[25] F.S. Billig. Research on Supersonic Combustion. *Journal of Propulsion and Power*, 9(4), John Hopkins University, Laurel, Maryland, July-August, 1993.

Annexes